Supplement of Atmos. Chem. Phys., 18, 17489–17496, 2018
https://doi.org/10.5194/acp-18-17489-2018-supplement

Atmospheric Chemistry and Physics
Open Access
EGU

Supplement of

Insignificant effect of climate change on winter haze pollution in Beijing

Lu Shen et al.

Correspondence to: Lu Shen (lshen@fas.harvard.edu)

Table S1. Correlations of the 2010-2017 $PM_{2.5}$ concentrations in Beijing in winter with an array of first principal components (PC1s) constructed using different combinations of meteorological variables and the predicted trends of winter $PM_{2.5}$ implied by these PC1s.

Experiment #	Variables	Correlation of PC1 with $PM_{2.5}$ (DJF, 2010-2017)	Predicted $PM_{2.5}$ Trend (DJF, 1973-2017, $\mu g\ m^{-3}a^{-1}$)	Predicted $PM_{2.5}$ Trend (DJF, 1993-2017, $\mu g\ m^{-3}a^{-1}$)
1	RH, V850	0.90	-0.12 (p=0.63)	0.001 (p=0.99)
2	RH, WS	0.88	-0.20 (p=0.37)	-0.64 (p=0.19）
3	RH, δU500	0.85	0.12 (p=0.59)	0.034 (p=0.93)
4	RH, V850, WS[a]	0.90	-0.21 (p=0.31)	-0.50 (p=0.27)
5	RH, V850, $\delta T_{925\text{-}1000hPa}$	0.91	NA[b]	-0.46 (p=0.33)
6	RH, V850, WS, $\delta T_{925\text{-}1000hPa}$, δU500	0.90	NA	-0.65 (p=0.13)
7	RH, V850, WS, $\delta T_{925\text{-}1000hPa}$	0.92	NA	-0.78 (p=0.10)
Average			-0.08 (p=0.71)	-0.43 (p=0.33)

[a] WS is for surface wind speed.
[b] Missing data because the observed $\delta T_{925\text{-}1000hPa}$ from radiosonde is available only after 1993.

Table S2. Models from the Coupled Model Intercomparison Project Phase 5 (CMIP5) used for this study.

Model Name	Institute
ACCESS1.0[a,b]	Commonwealth Scientific and Industrial Research Organization (CSIRO) and Bureau of Meteorology (BOM), Australia
ACCESS1.3[a,b]	CSIRO and BOM, Australia
BCC-CSM1-1[a,b]	Beijing Climate Center, China Meteorological Administration
BNU-ESM[a,b]	College of Global Change and Earth System Science, Beijing Normal University
CanESM2[a,b]	Canadian Centre for Climate Modelling and Analysis
CCSM4[a]	National Center for Atmospheric Research
CESM1-CAM5[a]	Community Earth System Model Contributors
CMCC-CM[a]	Centro Euro-Mediterraneo per i Cambiamenti Climatici
CMCC-CMS[a,b]	Centro Euro-Mediterraneo per i Cambiamenti Climatici
CNRM-CM5[a,b]	Centre National de Recherches Météorologiques / Centre Européen de Recherche et Formation Avancée en Calcul Scientifique
CSIRO-MK3-6-0[a,b]	Commonwealth Scientific and Industrial Research Organization in collaboration with Queensland Climate Change Centre of Excellence
FIO-ESM[a]	The First Institute of Oceanography, SOA, China
GFDL-CM3[a,b]	NOAA Geophysical Fluid Dynamics Laboratory
GFDL-ESM2M[a,b]	NOAA Geophysical Fluid Dynamics Laboratory
GFDL-ESM2G[a,b]	NOAA Geophysical Fluid Dynamics Laboratory
GISS-E2-H[a]	NASA Goddard Institute for Space Studies
GISS-E2-R[a]	NASA Goddard Institute for Space Studies
HadGEM2-AO[a]	Met Office Hadley Centre (additional HadGEM2-ES realizations contributed by Instituto Nacional de Pesquisas Espaciais)
HadGEM2-CC[a,b]	Met Office Hadley Centre (additional HadGEM2-ES realizations contributed by Instituto Nacional de Pesquisas Espaciais)
HadGEM2-ES[a]	Met Office Hadley Centre (additional HadGEM2-ES realizations contributed by Instituto Nacional de Pesquisas Espaciais)
INMCM4[a,b]	Institute for Numerical Mathematics
IPSL-CM5A-LR[a,b]	Institut Pierre-Simon Laplace
IPSL-CM5A-MR[a,b]	Institut Pierre-Simon Laplace
IPSL-CM5B-LR[a,b]	Institut Pierre-Simon Laplace
MIROC-ESM[a,b]	Japan Agency for Marine-Earth Science and Technology, Atmosphere and Ocean Research Institute (The University of Tokyo), and National Institute for Environmental Studies
MIROC-ESM-CHEM[a,b]	Japan Agency for Marine-Earth Science and Technology, Atmosphere and Ocean Research Institute (The University of Tokyo), and National Institute for Environmental Studies

MIROC5[a,b]	Atmosphere and Ocean Research Institute (The University of Tokyo), National Institute for Environmental Studies, and Japan Agency for Marine-Earth Science and Technology
MPI-ESM-LR[a]	Max-Planck-Institut für Meteorologie (Max Planck Institute for Meteorology)
MPI-ESM-MR[a,b]	Max-Planck-Institut für Meteorologie (Max Planck Institute for Meteorology)
MRI-CGCM3[a,b]	Meteorological Research Institute
NORESM1-M[a]	Norwegian Climate Centre
NORESM1-ME[a]	Norwegian Climate Centre

[a] The 32 models, each with monthly archives of meteorology.
[b] The 21 models, each with daily archives of meteorology.

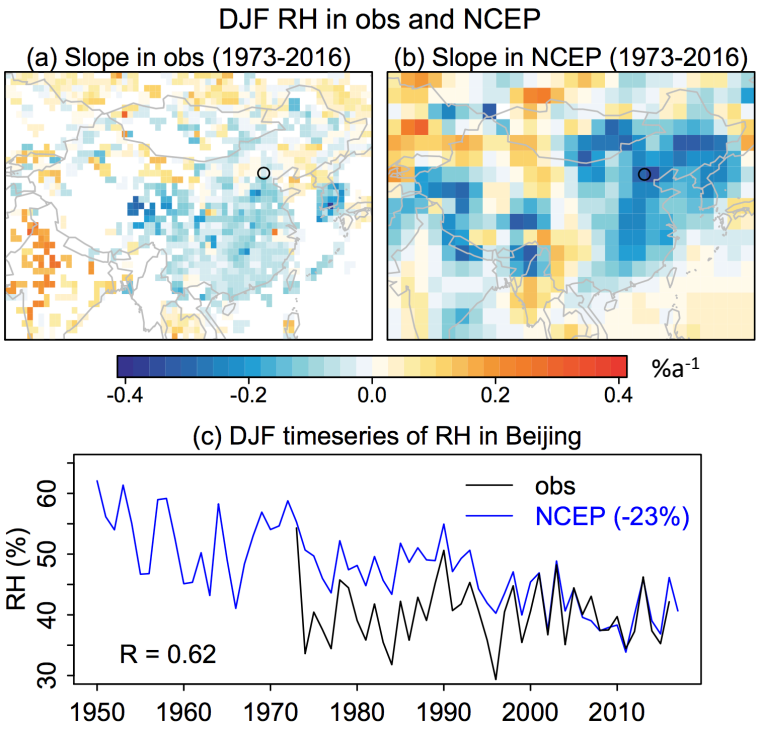

Fig. S1. Slopes of winter RH with reconstructed wintertime $PM_{2.5}$ concentrations in Beijing during 1973-2016 in (a) gridded global land and surface humidity dataset (HadISDH, https://www.metoffice.gov.uk/hadobs/hadisdh/) and (b) NCEP renanlysis. (c) Timeseries of mean DJF RH in Beijing from HadISDH and NCEP reanalysis. Because RH in the NCEP reanalysis is biased high, we reduce its magnitude by 23% in the plot.

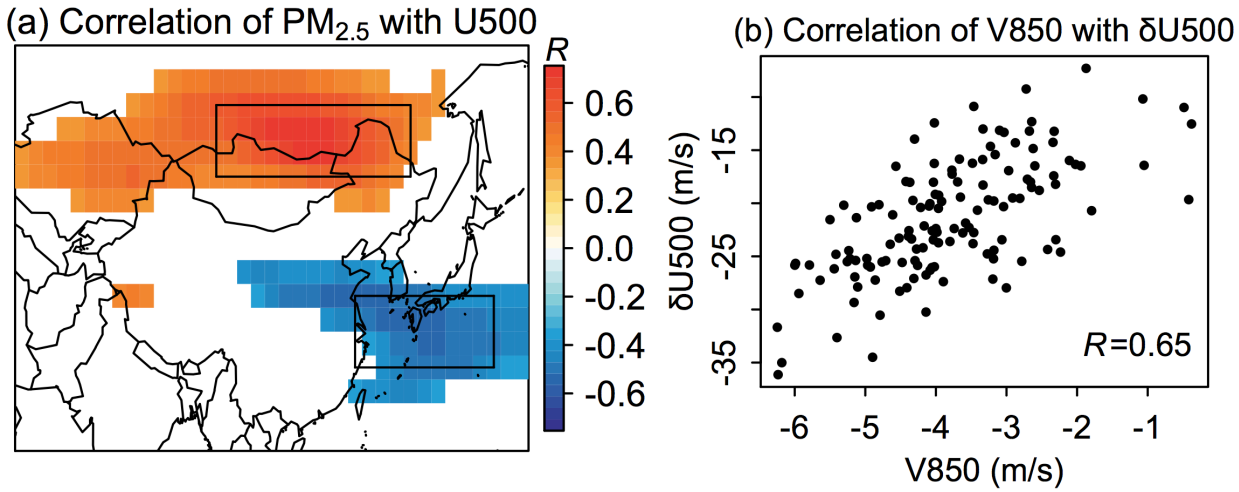

Fig. S2. (a) Same as Fig. 1a, but for the zonal wind speed at 500 hPa. We define δU500 as the difference between the mean zonal wind speed in the box north of Beijing (95°E-130°E, 47.5°N-55°N) and that in the box south of Beijing (120°E-145°E, 27.5°N-35°N). (b) Relationship of V850 and δU500 during winter months of 1973-2017, with the correlation coefficient shown inset.

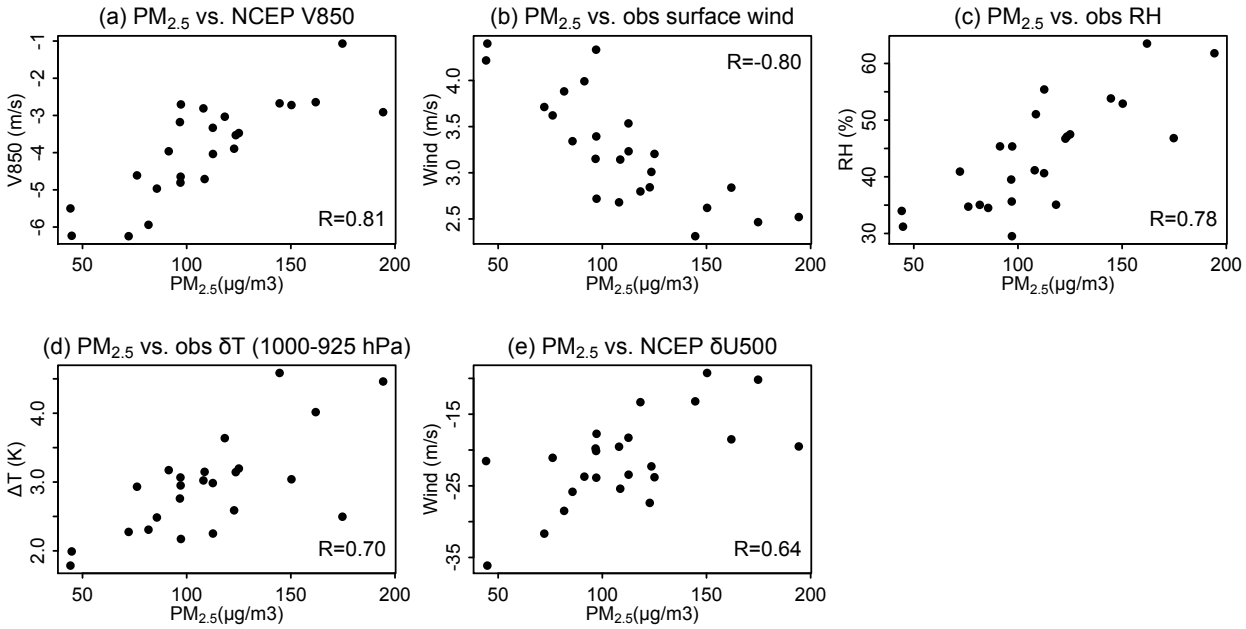

Fig. S3. Relationships of DJF monthly $PM_{2.5}$ concentrations with local and regional variables: (a) V850, (b) observed surface wind speed, (c) observed surface relative humidity, (d) potential temperature gradient between 925 and 1000 hPa, and (e) δU500. The correlation coefficients are shown inset. Definitions of V850 and δU500 are found in Fig. 1a and Fig. S3a.

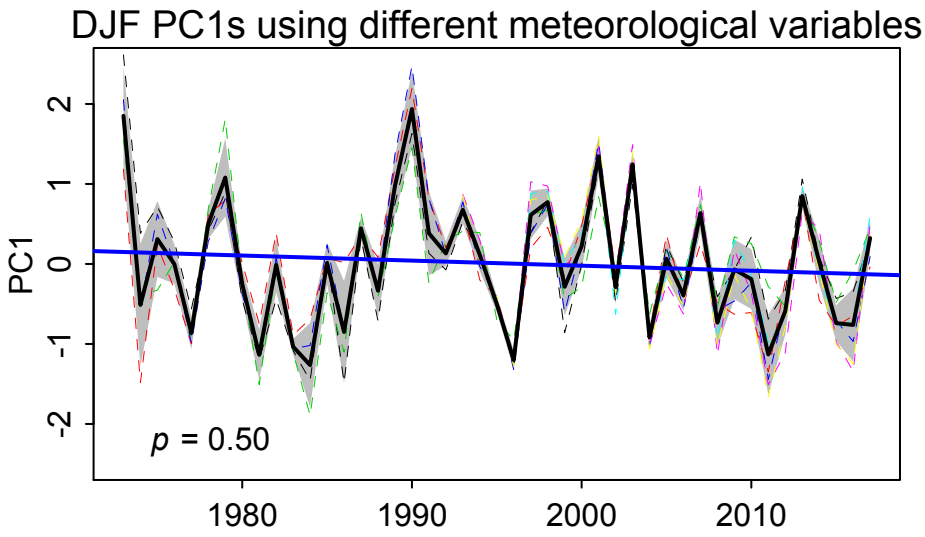

Fig. S4. Timeseries of PC1s calculated from seven different combinations of meteorological variables (dashed color lines). Details of these combinations are described in Table S1. The thick black line refers to the ensemble mean PC1. Shaded area denotes one standard deviation across ensemble members. The linear trend (blue line) of ensemble mean PC1 during 1993-2017 is insignificant ($p = 0.50$).

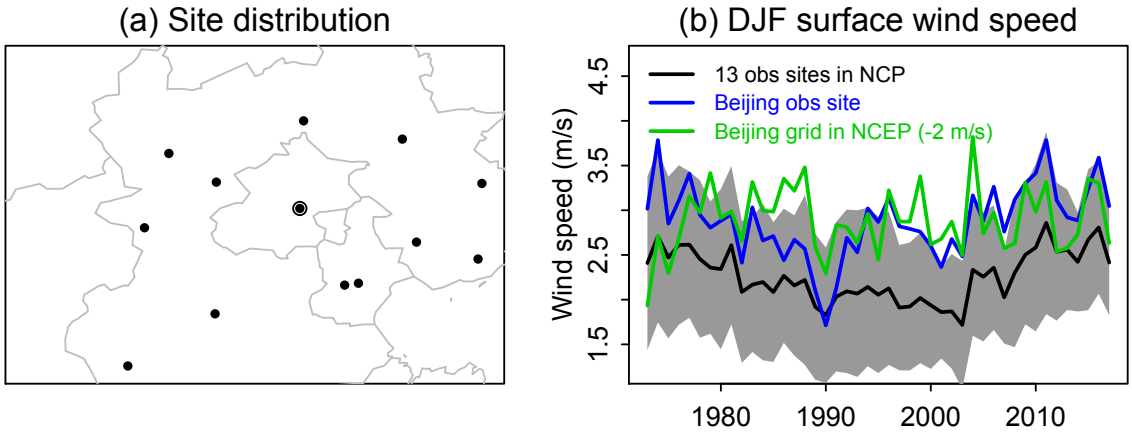

Fig. S5. (a) The geographical distribution of the 13 observation sites from the GSOD network used here. The Beijing site is highlighted. (b) Timeseries of 1973-2017 mean surface wind speed in winter at the Beijing site, the 13 sites in the North China Plain, and NCEP reanalysis. Because wind speed in the NCEP reanalysis is biased high in Beijing, we reduce its magnitude by 2 m s^{-1} in the plot.

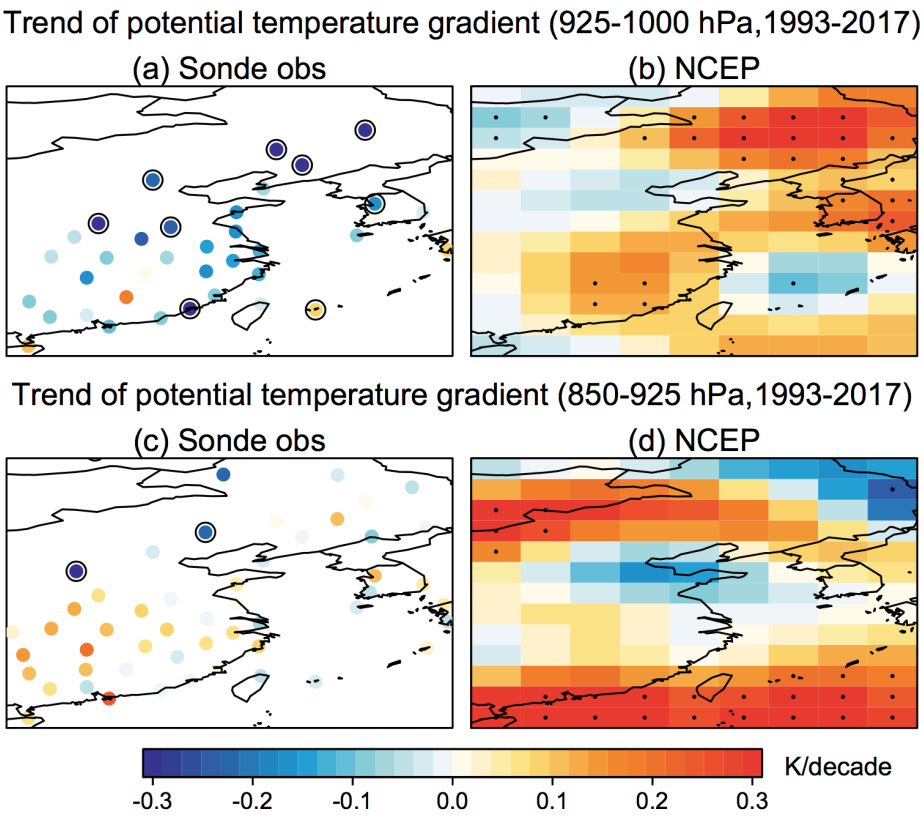

Fig. S6. (a) Observed trend of potential temperature gradient between 925 and 1000 hPa during the winters of 1993-2017. The sites with significant trend (p<=0.1) are circled. (b) Same as (a), but for the NCEP reanalysis. Gridboxes with significant trend (p<=0.1) are stippled. Panels (d-f) are same as (a-c), but for the trend of potential temperature gradient between 850 and 925 hPa.

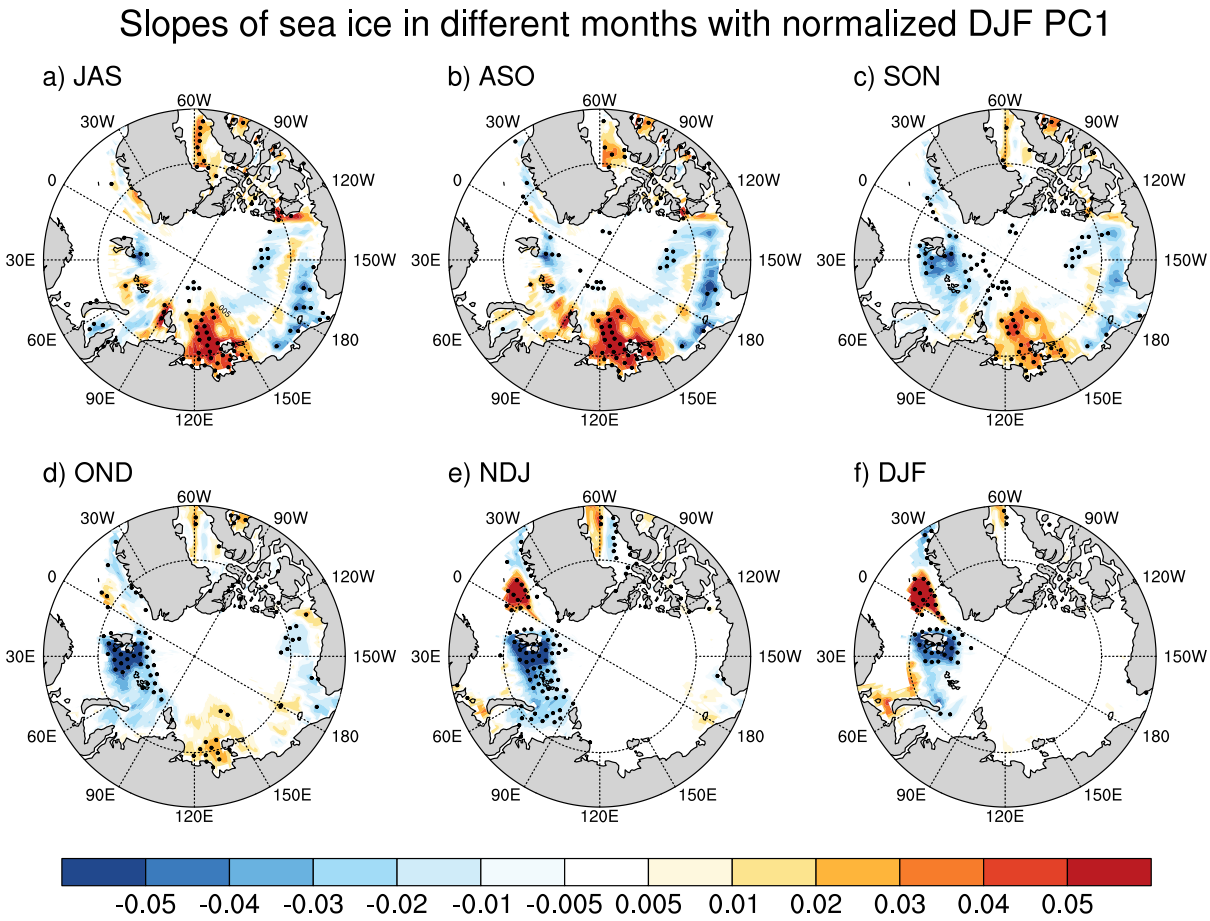

Fig. S7. Slopes of sea surface temperatures (SSTs) in the preceding months with DJF PC1 in Beijing during 1973-2017. Gridboxes with statistically significant correlations ($p<0.1$) are stippled.

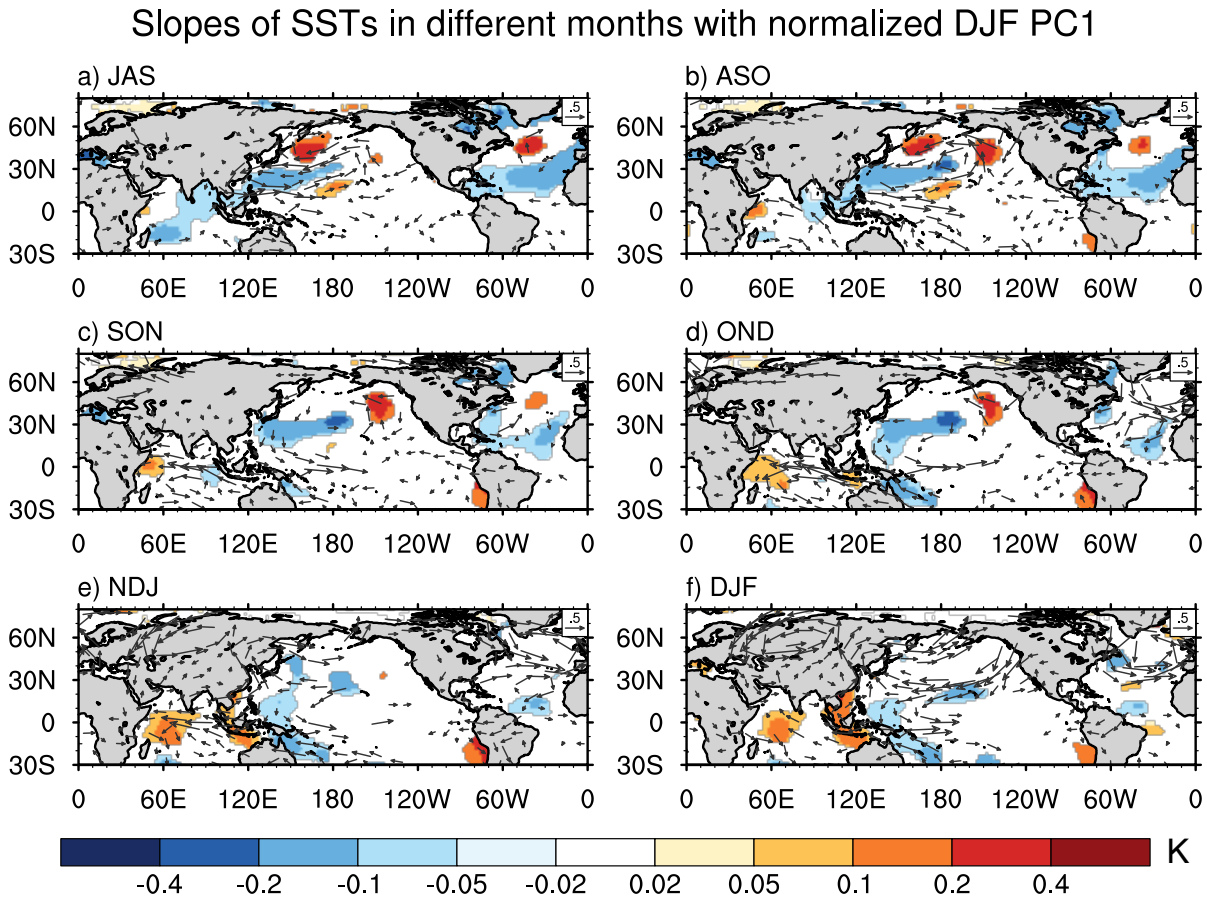

Fig. S8. Slopes of sea surface temperatures (SSTs) in the preceding months with DJF PC1 in Beijing during 1973-2017. Only regions with significant slopes are shown. The wind anomalies at 850 hPa relative to the 1973-2017 mean are overlaid.

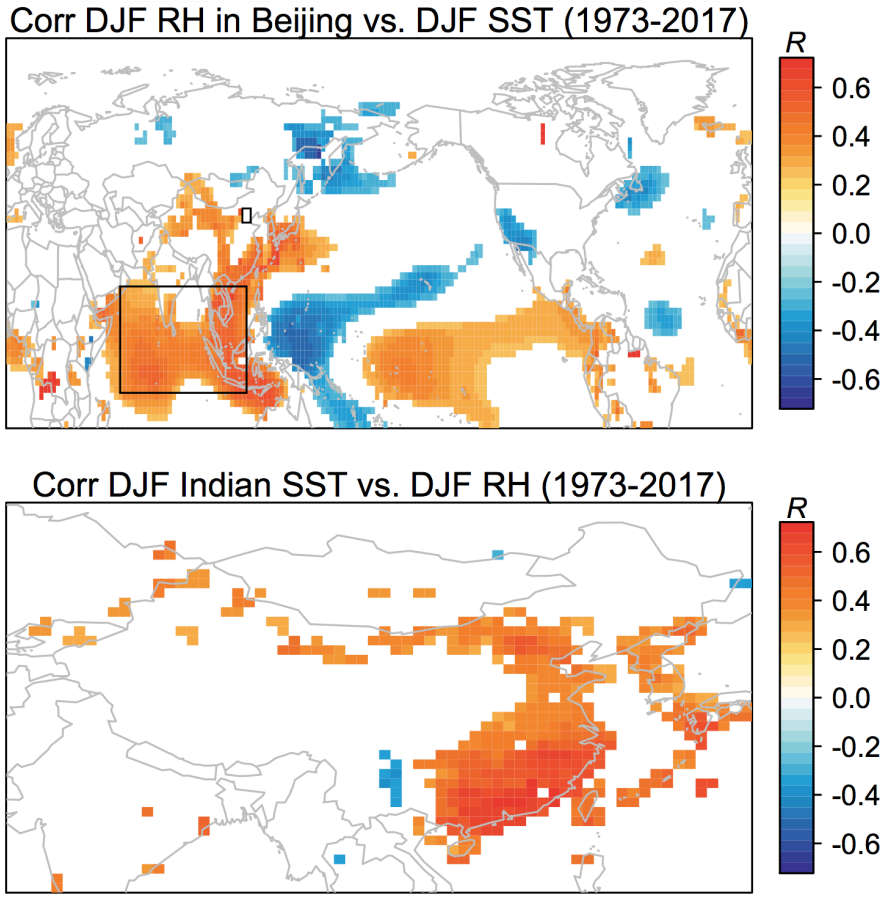

Fig. S9. (a) Correlations of DJF mean relative humidity in Beijing with DJF SSTs during 1973-2017. The black rectangle denotes the domain of Indian Ocean. (b) Correlations of mean SSTs in the Indian Ocean with relative humidity in East Asia. Only regions with significant correlations ($p<0.1$) are shown. All data are detrended by subtracting the 7-year moving average. The relative humidity is obtained from gridded global land surface humidity data (HadISDH, https://www.metoffice.gov.uk/hadobs/hadisdh/).

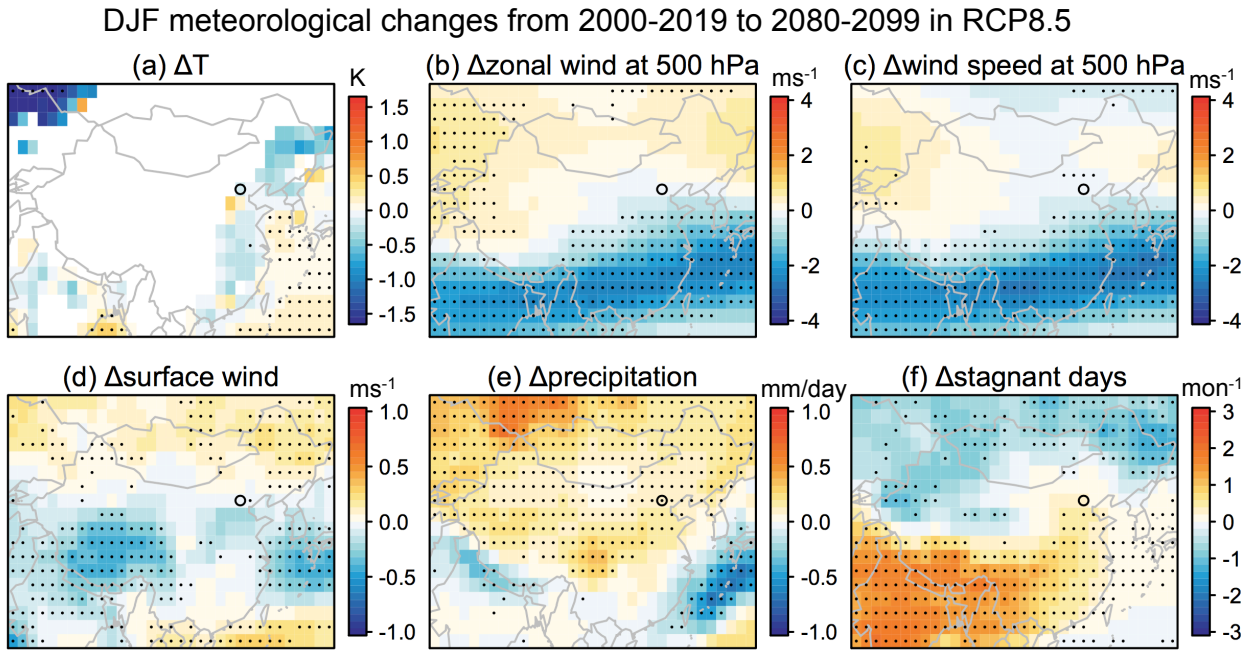

Fig. S10. Meteorological changes in DJF from 1970-1999 to 2079-2099 in the RCP8.5 scenario. These meteorological variables include (a) potential temperature gradient between 925 and 1000 hPa, (b) zonal wind speed at 500 hPa, (c) wind speeds at 500 hPa, (d) surface wind speeds, (e) precipitation, and (f) number of stagnant days. Gridboxes where more than 70% of the models show a consistent sign of changes are stippled. For panels (a-b), we use the 32 climate models that provide monthly archives (Table S2). For panels (c-f), we use the 21 climate models that provide daily archives (Table S2). The open triangle is the location of Beijing. We classify a day as stagnant when the daily mean near-surface wind speed is less than 3.2 m s^{-1}, daily mean mid-tropospheric wind speed is less than 13 m s^{-1}, and daily accumulated precipitation is less than 1 mm (Horton et al., 2012).

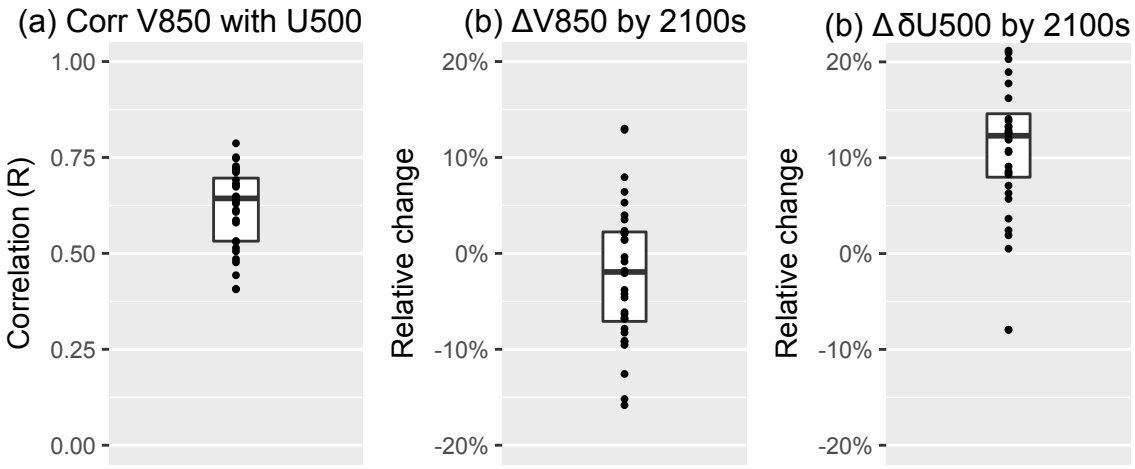

Fig. S11. (a) Correlation of V850 and δU500 in the winter months of 2000-2019 from an ensemble of 32 CMIP5 models. (b) The relative change of V850 from 2000-2019 to 2080-2089. (c) Same as (b) but for δU500.